Chapter 3

Experimental setup

3.1 Liquid crystals cells assembling and electrooptical observation

The ITO-coated glasses used as counter electrode in NLC cells are of two kind; one of them, were covered with polyimmide and underwent a rubbing process, to insure a better planar alignment of the NLC molecules. The other one consist of an ITO-coated glasses covered by a silica oxide film ever treated to ensure a planar alignment.
For the electrodes covered by the sol-gel solution, on the contrary, no surface treatment has been performed because the rectification effect is supposed to be related to the charge distribution at the oxide-liquid crystals interface. Thus, the insertion of an alignment layer could strongly modify the wanted phenomena. Moreover, the oxide layer induced a homogeneously planar alignment of the liquid crystal molecules (**n** parallel to the boundary surfaces) in all the prepared cells.

The two plates were closed in the standard sandwich configuration by using metallic clamps. The thickness of the cells was ensured by stripes of Mylar (8 μm), and the final value was deduced by analyzing the interference patterns in the transmittance spectrum of the empty cell, measured by a spectrophotometer.
The introduction of the liquid crystal in the space enclosed between the asymmetric glass plates was made very slowly to prevent any orientational alignment induced by the flow. The cell was filled with a NLC called *BL001* by Merck (former E7). The temperature range of existence for the nematic mesophase is from 20°C up to 61°C and the dielectric anisotropy $\Delta\varepsilon=\varepsilon_{//}-\varepsilon_{\perp}=+13.8$ (at 20°C). Observations of the electro-optical response of the cells, between crossed polarizers, were made by a polarizing microscope Axioskop Pol (Zeiss). The starting orientation of the NLC cell is set in such a way to have a maximum of the transmitted light, when placed on the stage of the microscope between crossed polarisers. Videomicroscopy was performed by a 3CCD color camera TCM 112 (GDS Elettronica) connected to a PC equipped to visualize and to capture the images of the samples. The investigation of the transmitted light intensities was carried out by a large area silicon photodiode (Hamamatsu) mounted on the polarising

microscope. The electrical signal proportional to the light intensity was collected by a digital oscilloscope (Tektronics, Mod. TDS 7254) and saved in digital form for the subsequent processing. Electrical measurement of the current flowing trough the cells are also detected from a resistor connected in series to the NLC cells at the reference electrode (see fig1).

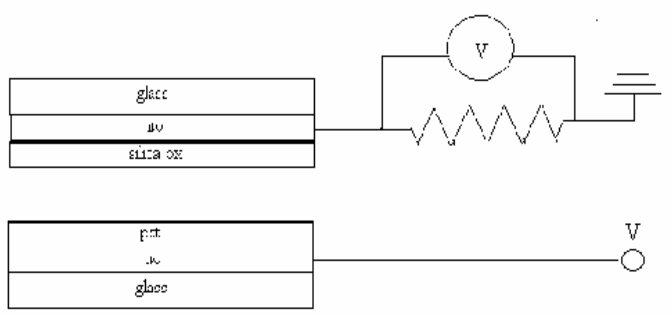

Fig3.2.1) Current measurements setup

3.2 Impedance measurements

From the impedence spectra of a sample is possible, not only to identify the equivalent circuit representing the conduction characteristics of the

analysed system, but also to attribute accurate numeric value to the circuital parameters. The measure consist of sending a sinusoidal signal of the kind $\vec{E} = E_0\sin(\omega t)$ to the sample in which ω is the angular frequency and E_0 the amplitude of the signal. For such exciting field correspond a current response of the kind $I = I_0\sin(\omega t + \phi)$, where I_0 is the current amplitude and ϕ the phase. Now the impedance of the sample can be represented in complex form by the usual formula

$$\vec{Z}(\omega) = \frac{\vec{E}}{\vec{I}} \qquad 3.2.1)$$

If the analysed samples are identifiable as resistive or reactive elements, the response of the system, in function of the applied frequencies, is described by the movement of the vector $\vec{Z}$,of module $Z_0 = E_0/I_0$ and phase ϕ, in the plane Im(Z)-Re(Z) (see fig. 3.3.1). in Cartesian coordinates the total impedance is obtained by adding the real part and the imaginary part $\vec{Z}(\omega) = \mathrm{Re}\,\vec{Z} + \mathrm{Im}\,\vec{Z}$ where $\mathrm{Re}\,\vec{Z} = Z_0\cos(\phi)$ and $\mathrm{Im}\,\vec{Z} = Z_0 sin(\phi)$. Moreover are also valid the equations

$$Z_0 = \left(\mathrm{Re}\, Z^2 + \mathrm{Im}\, Z^2\right)^{\frac{1}{2}} \qquad 3.2.2)$$

$$\phi = \mathrm{arctg}\ \frac{\mathrm{Im}\ \vec{Z}}{\mathrm{Re}\ \vec{Z}} \qquad 3.2.3)$$

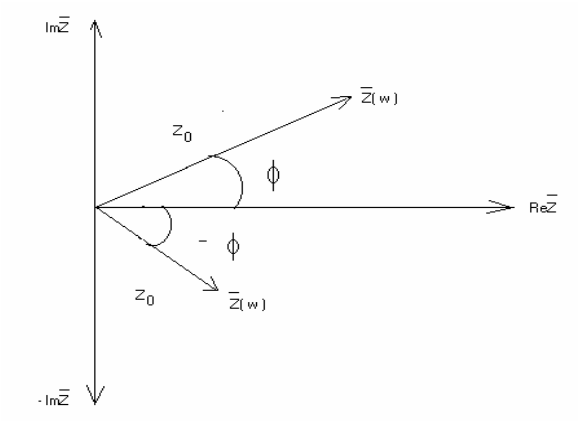

Fig. 3.2.1) Rotative vector $\vec{Z}$ *in the complex plain*

In the case of pure resistive elements, there is not phase displacement between current and voltage ($\phi = 0$) and the vector $\vec{Z}$ shift along the real axes, in the case of inductive elements ($\phi>0$) $\vec{Z}$ is moving on the 1° square while, in the case of capacitive elements, $\vec{Z}$ 4° square. Hear, for convenction, the position of $\vec{Z}$ on the 4° square is shifted on the 1° square and the $-\mathrm{Im}\vec{Z}$ value are associate to the positive y half-axis. In fig. 3.3.2 is showed, as example, the behaviour of $\vec{Z}$ for a parallel R-C circuit

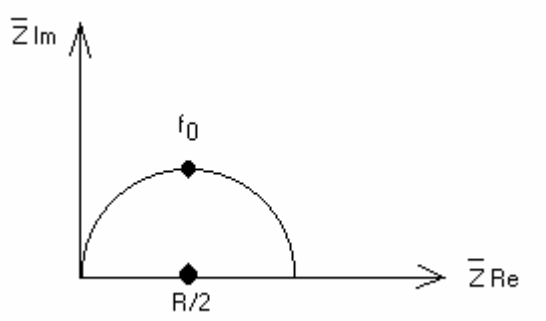

Fig. 3.2.2) Impedance spectra of a parallel R-C circuit

In this work the experimental setup for the impedance measurement is constituted by a lock-in amplifier princeton applied research 5210 used for the frequency sweep, a conductibility bridge

Potentiostat/galvanostat/impedentiometer EG&G 273A and a differential electrometer. The voltage response tacked to the heads of the sample is send back to the look-in so that to bee vectorially read. Subsequently is sent to a PC through the conductibility bridge so that to visualize and acquire the real and imaginary component. The sample is connected to the differential electrometer that serves as interface with the galvanostat. Moreover the electrometer checks the potential through the reference interface.

3.3 Calorimetry

The objective of the calorimetry is to measure the heat exchange between thermodynamic systems. Chemical reactions and physical transitions are related with heat dissipation or heat absorption and the calorimetry is a useful method to investigate such process. When a system is heat absorbing, according to the transformation that is had, its temperatures can vary or not vary. If the temperature of the system passes from T_i to T_f during an heat absorption, we define thermal capacity the quantity

$$C = \frac{\delta Q}{dT} \qquad 3.3.1)$$

The thermal capacitance per mass unity is called "specific heat" and it is measured in $JK^{-1}g^{-1}$. The thermal capacitance can bee negative, zero, positive or infinite according to the transformation of the system during the heat exchange. In this work, the thermal capacitance measurements, has been used as characterisation of PZT thin films.

Calorimetric measurement has been effected with a Perkin-Elmer Pyris Diamond DSC calorimeter (power compensation DSC). The main property of power compensation DSC calorimeter consist in the use of two measurement systems ideally identical (sample and reference) and isoperibolic, submitted to the same temperature controlled program; what is effectively measured is the difference of heat flow between the furnace containing the sample and those containing the reference. The furnace are separately heated so that to follow the temperature-time program. In first approximation external troubles will have the same effect on both the measurement systems therefore they will annul him. During an heating cycle the same power is furnished to both the furnaces by a control circuit,

so that to maintain their average temperatures in accord with the planned heating program. If there is an ideal symmetry the temperatures of both furnaces is always the same. This is verified if the two furnaces are perfectly identical and the sample is identical to the reference. When an asymmetry occur, for instance as a result of a reaction of the sample, a difference of temperature between the furnace in which is lodged the sample and that it contain the reference is observed. If, for example, an esothermic or endothermic transformation of the sample happens, the device must compensate the surrendered or purchased heat by the sample subtracting or furnishing a quantity of heat equal to that produced during the transformation. The electric power applied to the furnace containing the sample is regulated by a proportional control so that such power is increased or decreased according to that produced or consumed during the transformation. In this way the power compensation DSC measures the difference of heat flow to furnish to the sample respect to the reference so that the two system perform the same temperature program, is that, between the two system is maintained a temperature difference peer to zero. The measured signal is, therefore, the temperature difference ΔT (deviation from the planned value) to which the compensation power ΔP is proportional:

$\Delta P = -k_1 \Delta T$ [Hemminger et al., 1984]. The temperature difference between the sample and the reference is both the measured signal and the input of a second control circuit; this last compensates the heat flow by a proportional control which increases or decreases the thermal power furnished to the sample. Such thermal compensation power ΔP is proportional to the temperature difference ΔT. The relationship between ΔP, ΔT and the measured heat flow Φ_m are:

$$\Delta P = -k_1 \Delta T$$

$$\Phi_m = -k_2 \Delta T$$

where k_1 it is a coefficient fixed by the control circuit, while k_2 can be adapted by softwere (calibration). [1]

3.4 Raman spectroscopy

Since the discovery of the Raman scattering in the 1928 a huge number of related reports and monographs have been written regarding the

theories, instrumentations, applications and interpretations of the spectra [2-3].

When a radiation, monochromatic of frequency ω_1 is incident on a material, some "part" of the radiation is transmitted, some reflected and some scattered. The scattered radiations may show three kind of frequencies (ω_s): ω_1 and $\omega_1 \pm \omega_M$, where ω_M are the frequencies of some transitions which occur in the material.

The scattering without change of frequency is called Rayleigh and it is also said elastic scattering whereas the scattering that depends on the transitions of the material is called Raman scattering or inelastic scattering.

In the Raman scattering the lines or bands with frequencies lower than the frequency of the incident radiation are called Stokes while those with increased frequencies are called anti-Stokes.

In both classical and quantum models the origin of the scattered radiation is attributed to the oscillating electric dipole moments induced by the incident electromagnetic radiation. The contributions of the oscillating magnetic dipole and electric quadrupole are several order of magnitude smaller with respect to the dipole electric contribution, and for this reason they will not be considered in this treatment.

The intensity (I) of the scattered radiation radiated by an oscillating electric dipole induced by the

electrical field of the radiation incident (ω_1) is given by:

$$I = \frac{\omega_s^4 p_0^2 \sin^2\theta}{32\pi^2 \varepsilon_0 c_0^3} = \frac{\pi^2 c_0 \tilde{\nu}_s^4 p_0^2 \sin^2\theta}{2\varepsilon_0} \qquad 3.4.1)$$

where ω_s $\left(\omega_s = 2\pi c_0 \tilde{\nu}_s\right)$ and p_0 are the frequency and the amplitude of the induced electrical dipole and θ is the angle between the electrical field of the radiation and the axis of the dipole.
The induced electric dipole moment vector $\vec{P}$ (time dependent) is linearly dependent on the electric field $\vec{E}$ of the incident radiation:

$$\vec{P} = \vec{\alpha}\vec{E} \qquad 3.4.2)$$

where $\vec{\alpha}$ is the polarizability tensor, that is a II rank tensors.
Let consider just one molecule that is able to vibrate only (it cannot rotate). In this case, the polarizability can be modified during the molecular vibration and so the variation of the polarizability can be expressed by expanding each component

(α_{xy}) of the polarizability tensor in a Taylor series with respect to the normal coordinates of vibration:

$$\alpha_{xy} = (\alpha_{xy})_0 + \sum_k \left(\frac{\partial \alpha_{xy}}{\partial Q_k}\right)_0 Q_k + \frac{1}{2}\sum_{k,l}\left(\frac{\partial^2 \alpha_{xy}}{\partial Q_k \partial Q_l}\right)_0 Q_k Q_l + \ldots \quad 3.4.3)$$

where $(\alpha_{xy})_0$ is the value of α_{xy} at the equilibrium configuration and Q_k, Q_l are normal coordinates of vibration associated with the molecular frequencies ω_k, ω_l and the summations are over all the normal coordinates.
In "harmonic approximation" the eq. 3.1.3 is taken with the term that involve only the first power of Q. The eq. 3.4.3 can be rewritten as:

$$(\alpha_{xy})_k = (\alpha_{xy})_0 + (\alpha'_{xy})_k Q_k \qquad 3.4.4)$$

where

$$(\alpha'_{xy})_k = \left(\frac{\partial \alpha_{xy}}{\partial Q_k}\right)_0 \qquad 3.4.5)$$

The $\left(\alpha'_{xy}\right)_k$ are the components of a new tensor $\vec{\alpha}'_k$ called derived polarizability tensor because all its elements are polarizability derivatives with respect to the normal coordinate.
Therefore, the eq. 3.4.4 in vector form becomes:

$$\vec{\alpha}_k = \vec{\alpha}_0 + \vec{\alpha}'_k Q_k \qquad 3.4.6)$$

The scalar quantity Q_k, in the harmonic approximation, is given by:

$$Q_k = Q_{k_o} \cos(\omega_k t + \delta_k) \qquad 3.4.7)$$

where Q_{k_o} is the amplitude of the normal coordinate and δ_k is a phase factor.
The frequency dependence of the electric field of the incident radiation can be given by:

$$\vec{E} = \hat{E}_0 \cos \omega_1 t \qquad 3.4.8)$$

Substituting, the eq. 3.4.7, into eq. 3.4.6 and then taking in account the eq. 3.1.8 the eq. 3.4.2 can be written as:

$$\vec{P} = \vec{\alpha}_0 \hat{E}_0 \cos\omega_1 t + \frac{1}{2}\vec{\alpha}'_k \hat{E}_0 [\cos(\omega_1 t + \omega_k t + \delta_k) + \cos(\omega_1 t - \omega_k t - \delta_k)] \quad 3.4.9)$$

where the term $\vec{\alpha}_0 \hat{E}_0 \cos\omega_1 t$ represents the "classical" Rayleigh scattering, whereas the others two terms $\frac{1}{2}\vec{\alpha}'_k \hat{E}_0 \cos(\omega_1 t + \omega_k t + \delta_k)$ and $\frac{1}{2}\vec{\alpha}'_k \hat{E}_0 \cos(\omega_1 t - \omega_k t - \delta_k)$ are indicating the anti-Stokes and Stokes bands of the Raman scattering, respectively.

It can be noticed that the Rayleigh scattering has the same phase of the incident radiation while the Raman scattering does not: the quantity δ_k defines the phase of the normal vibration Q_k respect to the electrical field. Raman scattering arise from electric dipole oscillating at $\omega_1 \pm \omega_k$ frequencies that are produced when the electrical dipole oscillating at frequency ω_1 is modulated by the "system" oscillation at frequency ω_k. Indeed, Rayleigh scattering come up by the oscillation at ω_1 of the electric dipole induced by the electrical field of the

incident radiation and where ω_1 represents the frequency of the electrical field.

The necessary condition for obtaining Raman scattering is that at least one component of the derived polarizability tensor $\vec{\alpha}'_k$ be non-zero. From eq. 3.4.5, each component $\left(\alpha'_{xy}\right)_k$ of the derived polarizability tensor $\vec{\alpha}'_k$ is the derivative of the corresponding component of the polarizability tensor with respect to the normal coordinate of vibration Q_k in its equilibrium position. Therefore, the condition for Raman activity is that, for at least one component of the polarizability tensor the gradient with respect to the normal coordinate, in its equilibrium position, must be non-zero.

It is wanted to remember, that in order to obtain the eq. 3.4.9, the harmonic approximation has been done. Actually, if the mechanical anharmonicity is considered, the time dependence of the normal coordinate Q_k (eq. 3.1.7) will include terms as $\cos(2\omega_k t + \delta_{2k})$, $\cos(3\omega_k t + \delta_{3k})$ and so on, which produce bands called overtones and may be also terms as $\cos(\omega_k t + \delta_{kl})\cos(\omega_l t + \delta'_{kl})$ which produce combinations tones. The resulting induced electric dipoles will oscillate with additional frequency terms as $\omega_1 \pm 2\omega_k$ etc, and $\omega_1 \pm (\omega_k \pm \omega_l)$ etc.

Let us now to consider the Raman effect in the solids. In solid system the reticular vibration or elastic wave is quantized[4-5]. As well as for the electromagnetic wave the energy quantum is the photon for the reticular vibration the quantum of energy is called phonon. Nearly all the concepts developed for photon are valid for the phonon, for example: the wave-particle duality, and so on.

Let be, as above, a monochromatic light beam of frequency ω_1. The light will propagate with the propagation vector $\vec{k}_1$, $\left|\vec{k}_1\right| = \omega_1 \cdot \eta(\omega_1)/c_0$ where $\eta(\omega_1)$ is the refractive index.

The propagation vector of the scattered light is $\vec{k}_s$, $\left|\vec{k}_s\right| = \omega_s \cdot \eta(\omega_s)/c_0$.

Thus, it is possible to define the scattering frequency as:

$$\omega = \omega_1 - \omega_s \qquad 3.4.10)$$

and the scattered wave vector as

$$\vec{k} = \vec{k}_1 - \vec{k}_s \qquad 3.4.11)$$

In order to have Raman scattering the conservation of the energy and of the moment laws (eqs. 3.4.10-3.4.11) must be satisfied.

In a perfect crystal the elementary excitations (phonon) are represented by the wave vector $\vec{q}$ and frequency ω_q, connected by a dispersion relation that specifies a frequency ω_q for each value of $\vec{q}$.

In the first order process only one elementary excitation will take place and thus the scattered wave vector as well the scattering frequency will be equals to $\vec{q}$ and ω_q respectively.

For typical visible –near infrared set up the maximum phonon wave vector excited by the light has an order of magnitude $\cong 10^4\ cm^{-1}$ that is much smaller (about three order of magnitude) of the wavevectors corresponding to the Brillouin zone boundary of typical crystals ($\cong 10^7\ cm^{-1}$). Thus, for first order process that conserves the wave vector only elementary excitations close to the centre of the Brillouin zone must be considered. This, means intuitively, $\vec{q} \cong 0$, thus the incident radiations "sees" the many unit cells of a perfect crystal to vibrate in phase.

This allows to evaluate the symmetry of the vibrations by considering the point group symmetry

of the unit cell instead of the space group symmetry, treating the unit cells as molecules, with the consequent reduced difficulty because the point groups are just 32 while the space group are 230.
The theoretical treatment of the Raman effect on solid crystalline systems can, therefore, be deal with the above exposed theories.
In imperfect crystals, with a small concentration of defects, as well as in solid solution or in amorphous solids the conservations of the wave vector is not anymore respected and Raman spectra display such features, reflecting the density of the states of the particular excitation and this aspect make the Raman spectroscopy to play a fundamental role in the characterization of such systems.
However, the condition of the conservation of the wave vector has to be studied with some attention when the systems are constitute by quantum structure such as artificial multilayer systems which display size quantization along one or more directions.
The size quantization, also known as confinement, occurs when there is a small characteristic length, so that along that direction the motion is quantized into distinct energy levels, as in a quantum well: for electrons typical lengths are in the nanometers range and the structures are said nanostructures.
For example, let consider a binary alloy system as an perfect host crystal that contains some

impurities, with the same valence but with smaller mass than atoms of the host crystal, that have their own local vibrational modes often seen by Raman spectroscopy. From an atomic point of view, the heavier host atoms cannot follows the motion of the faster impurities. This results as a narrow band in the Raman spectra, because the local frequency mode associated to the light impurities will be well above the local frequency mode of the host crystal: so they cannot couple directly. Otherwise, if the impurities are heavier then the atoms of the host crystal the mode will not be anymore “local”, since the coupling occurs and the Raman band associated to that mode will be much broader then before.

The Raman spectra collected on amorphous materials will generally consist in broad bands with maxima approximately close to the frequency of the same mode of the materials in the crystalline phase, that shows a narrow bands. For this reason, Raman spectroscopy is a useful tools in order to study the structural phase transitions. Most studies show effects, on the materials, due to thermal or pressure treatment that usually are opposite: the increases of the temperature tends to increase the inter atomic distance while the increase of the pressure tends to reduce that.

Part of the experimental research presented in this thesis regards, in fact, the study of thin films (tungsten trioxide) obtained by different techniques

and to evaluate the effects of different thermal treatments at which they have been subjected.
As experimental setup a Raman microprobe Jobin-Yvon Labram was used equipped with a CCD detector and a He-Ne laser (632.8 nm emission). In all the experiments the power of the laser out of the objective (a 100x Mplan Olympus with Numerical Aperture of 0.90) was about 5 mW, and the focused laser spot had about 2-3 μm of apparent diameter. By assuming such values of spot diameter and laser power, we have for the unfiltered laser beam an irradiance of the order of 50-100 kW/cm^2 on the spot. To avoid unwanted laser-induced crystallizations, proper neutral filter were often used, having Optical Density 3, 2, 1, 0.6 and 0.3, corresponding to transmitted laser power fractions of 1/1000, 1/100, 1/10, 1/4 and 1/2, respectively. A special X-Y stage for automatic spectral mapping was used. The distances between the center of any spot and the next one on the line were of about 5 μm, to avoid overlapping of the heated regions (the gaussian spatial distribution of the light intensity in the laser beam insures that points close to the diameter assumed above have a real light intensity quite lower than in the center of the spot). The typical Raman spectra reported in the present work are extracted from such mapping.

References.

[1] G. Bellavia, A. Cupane: *studio calorimetrico di soluzioni acqua-glicerolo: effetto dell' incapsulamento in idrogel di silice e della presenza di mioglobina.*

[2] R. L. McCrerry, *Raman Spectroscopy for Chemical Analysis,* John Wiley & Sons, New York, (200)

[3] R. Loudon, *The quantum theory of light,* Oxford University Press, Oxford, (1973).

[4] C. Kittel, *Introduction to Solid State Physics,* John Wiley & Sons, New York, (1995).

[5] R. Merlin, A. Pinczuk and W. H. Weber, in *Raman Scattering in Material Science,* edited by W. H. Weber and R. Merlin, Springer, Berlin, (2000).